Journal of the Australian Ceramic Society (2020) 56:1397–1404
https://doi.org/10.1007/s41779-020-00480-2

RESEARCH

Co-dopants effect on translucent SiAlON ceramics production

Suna Avcioglu[1] · Semra Kurama[2]

Received: 6 October 2018 / Revised: 28 April 2020 / Accepted: 7 May 2020 / Published online: 3 June 2020

Abstract

SiAlON is a ceramic alloy (solid solution of Si_3N_4-Al_2O_3) which is discovered in the early 1970s. Since then, SiAlON ceramics have been used for structural applications due to its excellent fracture toughness and strength, outstanding chemical stability, and wear resistance. However, this material has also an enormous potential for functional applications. In this study, the effects of co-dopants on the IR transmittance of α-SiAlON ceramics were investigated. Compositions were designed by using two different cation combinations (Dy^{3+}-La^{3+}) and (Y^{3+}-La^{3+}). Starting powder mixtures were sintered by means of spark plasma sintering (SPS) technique. Microstructure and phase characterization of the samples was carried out by scanning electron microscope (SEM) and X-ray diffraction (XRD), respectively. The infrared transmission of α-SiAlON ceramics was measured by Fourier transform infrared spectroscopy (FTIR) in the range of 2000–7000 cm^{-1}. The results were discussed according to the relationship between density, phase composition, microstructure, and optical properties.

Keywords α-SiAlON · Additive cations · Microstructure · Optical properties · Infrared transmittance

Introduction

SiAlON is a kind of ceramic alloy (the solid solution of silicon nitride) which is produced by a combination of four elements (silicon (Si), aluminum (Al), oxygen (O), and nitrogen (N)). As a result of substitution for Si by Al with a corresponding atomic replacement of N by O, SiAlON has superior properties than Si_3N_4 such as high strength (even at high temperatures), good thermal shock resistance, and exceptional resistance to corrosion. SiAlON has two well-known phases, α- and β-SiAlON, based on the structure of α- and β-Si_3N_4 respectively. Furthermore, it is possible to fabricate ceramic materials with significantly improved fracture strength and toughness by a combination of hard α and tough β phase SiAlON [1]. So, SiAlON ceramics have been widely used for extremely harsh structural applications since the 1970s.

The general formula of α-SiAlON is M_x–$Si_{12-(m+n)}Al_{m+n}O_nN_{16-n}$ where M is one or more metal ionic, alkali, or rare earth. During the formation of α-SiAlON, Al substitution for Si is accompanied by interstitial M filling. Due to this reason, in comparison with β-SiAlON, additive oxides cause a reduced amount of grain boundary phase in α-SiAlON ceramics. The solubility of an additive cation in α-SiAlON tends to decrease with an increase in its size. Previous studies reveal that smaller interstitial cations promote the formation of single-phase α-SiAlON [2]. Lanthanum oxide (La_2O_3) was used as a sintering aid to produce Si_3N_4 and SiAlON ceramics [3, 4]. Even though lanthanum is the largest rare-earth cation, it has been reported that coupling lanthanum with calcium or ytterbium can promote the formation of α-SiAlON phase [4].

In addition to the stabilization of α-SiAlON phase, additive oxides were used to improve densification behavior and tailor final morphology of SiAlON ceramics. Even though α-SiAlON grains tend to form in equiaxed morphology, some published studies show that elongated α-SiAlON grains can form where the amount of transient liquid is high and the viscosity of the liquid is low [5]. Huang et al. observed elongated grain formation in α-SiAlON ceramics co-doped with Li-Y and Ca-Y [6]. Shen et al. also found that rare-earth interstitial cations with an atomic weight such as Nd and Sm promoted the formation of elongated α-SiAlON grains [7]. Wei et al. tailored α-SiAlON final morphology and mechanical properties by co-doping with Yb and Lu. According to their results, Yb-α-SiAlON possessed equiaxed grains, while

✉ Semra Kurama
skurama@anadolu.edu.tr

[1] Department of Metallurgy and Materials Engineering, Ondokuz Mayıs University, Kurupelit Campus, 55139 Samsun, Turkey

[2] Department of Materials Science and Engineering, Eskisehir Technical University, Iki Eylul Campus, 26555 Eskisehir, Turkey

Table 1 Codes of sintered samples, sintering conditions, and resulting densities

Sample code	Heating rate (°C/min)	Cooling rate (°C/min)	Applied pressure (MPa)	Sintering temperature (°C)	Holding time (s)	Density (g/cm^3)
Dy/La2010	100	300	50	1600	75	3.54
Y/La2010	100	300	50	1600	75	3.40

elongated and equiaxed grains co-existed in Lu-α-SiAlON. So, Yb/Lu-α-SiAlON ceramics with enhanced hardness and toughness were obtained [1].

In recent years, it has been noticed by many researchers that α-SiAlON ceramics could be an alternative to available transparent ceramics used in the compulsory application areas. α-SiAlON ceramics with improved IR transmittance might potentially be used as high-temperature IR windows, plasma panels (PDPs), protective armors, infrared (IR) heat seeking devices for missile guidance systems, and IR night vision. Due to this reason, serious attention was taken to improve the IR transmittance of SiAlON ceramics without losing its superior mechanical properties.

IR and visible light transmission through a polycrystalline ceramic have been determined by the theoretical maximum transmission restrictions of the material as well as the amount of reflection on both surfaces, diffuse scattering (at pores, second phases as pores or microstructural components with different refractive index), and birefringent scattering (especially important for optically anisotropic structures) [8, 9]. In order to produce highly transparent SiAlON ceramics, the starting composition should be designed in a single-phase region and furthermore, full densification must be provided to eliminate diffuse scattering. Equiaxed grain morphology helps to improve the transmission by reducing scattering and absorption in the polycrystalline ceramics from the inhomogeneity and anisotropy of grains [1]. It is relatively easier to produce α-SiAlON ceramics with equiaxed grain morphology and less amount of grain boundary phase than β-SiAlON, so in previous studies, mainly α-SiAlON phase was chosen to fabricate translucent SiAlON ceramics. Karunatne et al. reported that they could produce semi-transparent and rare-earth doped α-SiAlON ceramics with a thickness of 100 μm [10]. Jones et al. have carried out studies on the optical properties of Lu-α-SiAlON ceramics [11]. Over the following years, the same researchers reported that translucent α/β-SiAlON ceramics could be produced by the SPS method [12]. Shan Yingchun et al. aimed at increasing the transmittance value of translucent Y-α-SiAlON ceramics through the optimization of sintering conditions [13]. Attempts to improve the transparency of the SiAlONs have occurred by using different sintering techniques such as spark plasma sintering (SPS), hot isostatic pressing (HIP), hot press (HP), and gas pressure sintering (GPS) [14–17]. However, in addition to the sintering technique and sintering conditions, as mentioned above, α-SiAlON phase stabilizer cations from the additive oxides influence the final morphology and densification behavior of SiAlON ceramics dramatically. Xiong et al. fabricated 0.5-mm-thick translucent Mg-doped α-SiAlON ceramics [18]. Feng et al. fabricated dual Y-Yb-doped α-SiAlON ceramic by hot pressing technique at 1900 °C [19]. In addition to aforesaid dopants, many others such as alkaline earth cations (Ca^{2+} and Mg^{2+}) or rare earths (Lu^{3+}, Nd^{3+}, Sm^{3+}, Tb^{3+}, Dy^{3+}) have been used as additives and their effects on the production of transparent α-SiAlON ceramics have been investigated [20–22]. The common output of these

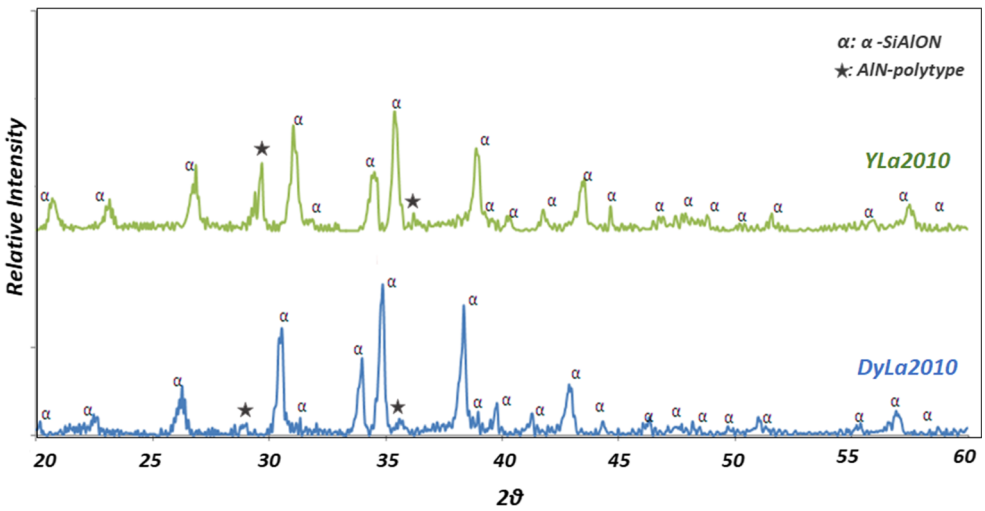

Fig. 1 XRD results of Y/La2010 (green) and Dy/La2010 (blue) samples

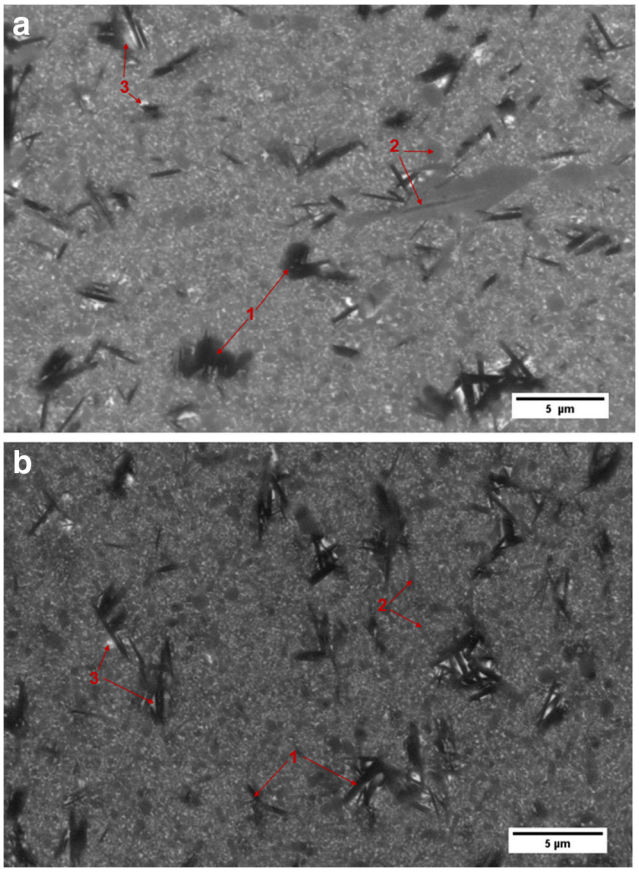

Fig. 2 Backscattered electron images obtained by scanning electron microscopy (SEM). **a** Dy/La2010 and **b** Y/La2010

studies suggests that compositional design, dopant type, and additive oxide amount are among the key factors to determine the morphological futures and the optical properties of α-SiAlON ceramics. Furthermore, dopants added in α-SiAlON structure also serve as the electrovalent balance cations and the valence shell of doped atoms interacts with the doping states of α-SiAlON, resulting in a change in the optical gap. Zhong et al. showed that doping of Dy, Y, and Gd atoms into the α-SiAlON can have a significant impact on the optical gap and electronic structure. Their results indicate that Dy doping, leading to an increase in the optical gap of α-SiAlON from 0.4 to 1.1 eV, improves the transparency in the infrared region from 1.5 to 4.5 μm [23].

However, among all these studies, not much work has been done on double cation doped translucent SiAlON ceramics, most of them generally focused on composition systems which include only one type of cation. Additionally, there is no other study in the literature reporting that La^{3+} is used as an additional additive for the production of translucent Dy- or Y-α-SiAlON ceramics. In this study, it was aimed to investigate the effects of co-doping Dy-La and Y-La on microstructural evolution and the infrared transmission of α-SiAlON ceramics. Besides, the influences of sintering additives on densification behavior and fabrication of translucent α-SiAlON ceramics by means of spark plasma sintering technique have been discussed.

Experimental procedure

Two different cation systems (Dy^{3+}-La^{3+}) and (La^{3+}-Y^{3+}) were selected to investigate the effects of sintering additives on the optical properties of α-SiAlON ceramics. Compositions were designed with respect to the general formula of α-SiAlON ($M_{(x)}Si_{12-(m+n)}Al_{(m+n)}O_{(n)}N_{(16-n)}$). For each cation system, value *m* and *n* in the formula were determined as 2 and 1, respectively. The starting powder mixtures were prepared by using (UBE-10, 1.6% surface oxide), AlN (Tokuyama, 1% surface oxide), Dy_2O_3 (Aldrich Chemical Co., 99.9% purity), La_2O_3 (Aldrich Chemical Co., 99.9 purity), and Y_2O_3 (Aldrich Chemical Co., 99.9% purity) commercial powders. The powder mixtures were ball milled (Pulverisette 6 Fritsch, Germany) in isopropanol alcohol for 1.5 h at 300 rpm using Si_3N_4 milling media. The prepared slurry was dried in a rotary drier after that dry powders were sieved using a 250-μm mesh sieve. The sintering of the samples was carried out using the spark plasma sintering (SPS) method (FCT GmbH, Germany). Three grams of powder mixture was put in a graphite-based mold than placed in the SPS furnace chamber without any other shaping process. During sintering, all sintering parameters were kept the same in both compositions and are shown in Table 1. The final densities of the sintered samples were measured by Archimedes' method. The microstructural analysis was carried out by means of a scanning electron microscope (SEM-Zeiss Supra 50V). EDX point analysis was carried out by using an Oxford Inca X-Act EDX detector attached to the SEM device. Infrared transmissions in wavenumber of 2000–7000 cm^{-1} were measured by FTIR (Bruker Tensor27). The phase composition of the sintered samples was analyzed using the X-ray diffraction method (Rigaku Rint 2200) with Cu K radiation ($\lambda = 1.540$ A) ° from 20°.

Results and discussion

The codes, the sintering conditions, and the measured density values of the α-SiAlON ceramics sintered with SPS technique are given in Table 1. According to the density measurement results, the density of both co-dopped α-SiAlON ceramic samples could reach about 98% theoretical density, while sintering process of SiAlON ceramics, oxide additives, and SiO_2 (the surface oxide of Si_3N_4) forms in a liquid phase by the eutectic reaction. Due to the reason that double oxide sintering additives were used in starting composition, fully densification was achieved with designed spark plasma sintering conditions. Doped system a small cation (Dy^{3+}) is used for stabilization of

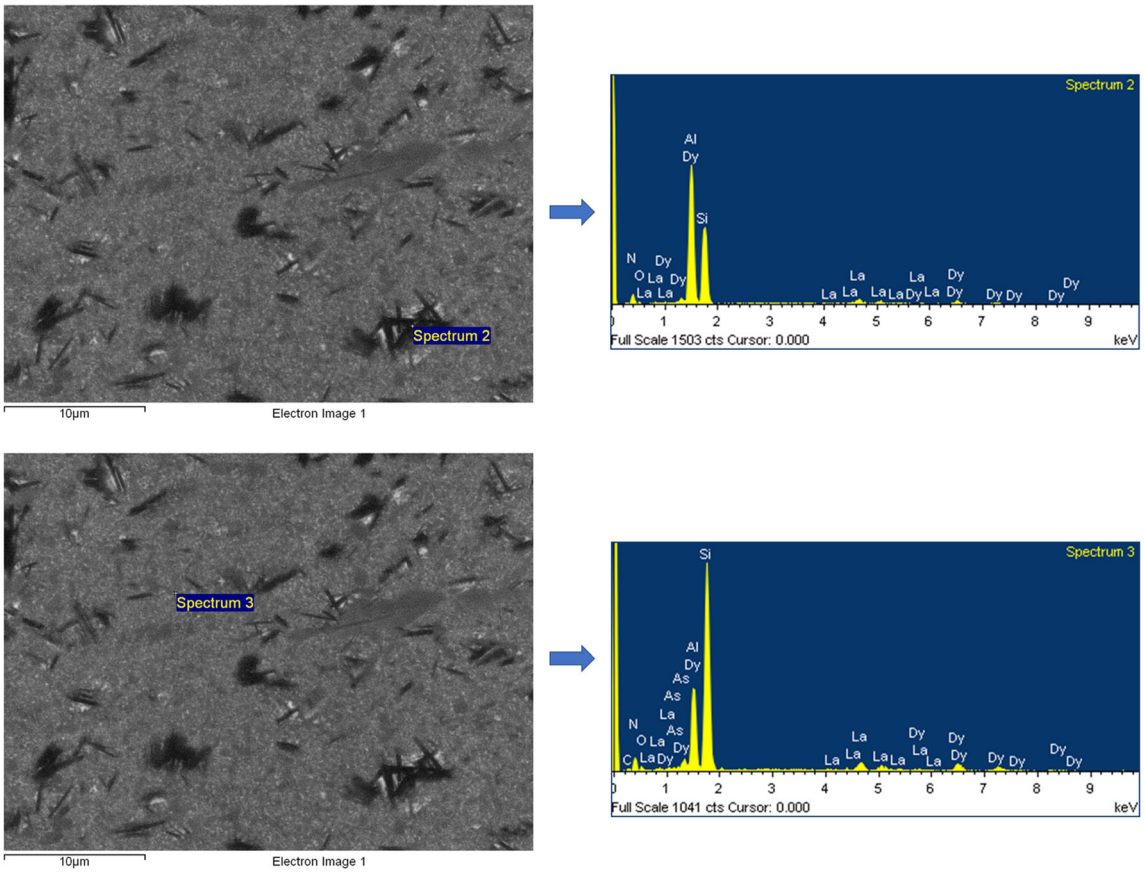

Fig. 3 The EDX analysis results of the AlN-polytype phase (spectrum 2) and α-SiAlON phase (spectrum 3) on Dy/La2010 sample

the large cation (La^{3+}) in α-SiAlON structure whereas La^{3+} has an important role in increasing the amount of liquid phase which helps the densification of sample. In the second system, Y^{3+}-La^{3+}, Y^{3+} has a role to stabilize the α-SiAlON phase and keep La^{3+} cation in its structure. Also, results are in agreement with these aims (Table 1 and Fig. 1).

The XRD analyses of the sintered samples were carried out to identify the phase compositions. X-ray diffraction patterns of the Y/La2010 and Dy/La2010 samples are shown in Fig. 1. The results show that α-SiAlON is the major phase in both samples. Besides the α-SiAlONs, two characteristic peaks of AlN-polytype phase were detected. It is well known that the formation of AlN-polytype phase is very common while fabricating α-SiAlON ceramics [24, 25]. During the fabrication of SiAlON ceramics, wetting behavior of the eutectic melt of M_2O_3–Al_2O_3–SiO_2 plays an important role in determining the reaction pathway. The melt with strong alkaline M element wets Si_3N_4 more easily than AlN. Therefore, the formation sequences of α-SiAlON and AlN-polytype could be controlled by using modifier ions. Eventually, the phase composition and microstructure of the α-SiAlON and AlN-polytype could also be influenced by the modifier ion [26–28]. Even though AlN-polytypes mechanical properties are relatively lower than α-SiAlON, because of its fiber-like morphology they have a potential to toughen α-SiAlON ceramics [29].

Also, the stability of α-SiAlON phase strongly relies on the ionic size of additive rare-earth cations. Lanthanum with relatively high ionic radius (r_{La}^{3+} = 1.06 Å) is not one of the rare-earth cations which can promote the formation of α-SiAlON by itself [4]. Due to this reason, using second α-SiAlON stabilizing rare-earth cation can be helpful to the formation of 100% α-SiAlON ceramics. As shown in Fig. 1, no β-SiAlON was not observed at XRD analysis results. So, by the aid of Dy^{3+} and Y^{3+}, α-SiAlON ceramics with a little amount of AlN-polytype were successfully fabricated.

Backscattered scanning electron microscopy (SEM) images of the SPS-ed Dy/La2010 and Y/La2010 samples are shown in Fig. 2(a) and (b), respectively. The first examination of SEM micrographs confirms the density measurement results. No porosity was detected on SEM micrographs, so it can be said that both samples were fully densified. It is clearly seen that both samples contain three different phases with

Table 2 Weight ratios of the elements (%) in the different phase zones

Type of element	N (%)	O (%)	Al (%)	Si (%)	Dy (%)	La (%)
Spectrum 2	31.98	6.63	11.88	35.64	5.93	8.22
Spectrum 3	33.72	4.94	27.91	24.20	4.95	4.28

Table 3 Measured transmission percentages at specific sample thickness

	Sample thickness (mm)						
	3	2.6	2	1.5	0.8	0.5	0.3
Transmission (%) of Dy/La2010	–	0%	0%	0%	1.8%	3%	7.79%
Transmission (%) of Y/La2010	–	0.13%	1.7%	2%	2.96%	11.6%	21.489%

different contrasts in the images. AlN-polytype phase with needle-like morphology has black color due to the reason that it does not incorporate any additive cation; in other words, its atomic number is relatively lower. AlN-polytype phase was marked with number 1 on the SEM images. The samples contain the equiaxed and little amount of elongated α-SiAlON grains. Because of the incorporation of additive cations into the α-SiAlON crystal structure, α-SiAlON grains are shown as gray colored. The phase shown as white-colored is the rare-earth cation-rich glassy phase and generally placed in triple pockets of α-SiAlON grains. Also, a high amount of glassy phase puddles observed between needle-like AlN-polytype grains. α-SiAlON grains and glassy phase marked with numbers 2 and 3 on SEM images respectively.

The EDX point analysis was carried out to determine the elemental distribution difference between the observed needle-like dark grains and equiaxed gray grains. The results were shown in Fig. 3. Needle-like AlN-polytype phase (spectrum 2) includes more amount of Al and a lower amount of additive cation than α-SiAlON phase (spectrum 3). It is observed that 35.64% at. Si exists at spectrum point 3, and on the other hand, only 24% at. Si found at spectrum point 2. That shows that α-SiAlON phase is richer than AlN-polytype phase with regard to the amount of Si element. In Table 2, the weighted percentages of the elements in the analyzed regions were given. The results indicate that α-SiAlON phase reached the Al solubility limit for the composition of $m = 2$, $n = 1$, so the formation of AlN-polytypoids was observed.

Sintered sample thicknesses were reduced for infrared transmission measurements by means of rough ceramic grinding and surface polishing up to 0.3 mm. Because a certain relationship exists between transmission and thickness of material which is known as Beer-Lambert Law (Eq. 1), FTIR measurements were carried out between 1000 and 7000 cm^{-1} wavenumber region at different sample thickness multiple times for each sample.

The general Beer-Lambert law is usually written as in Eq. 1, where A is the measured absorbance, ε is the wavelength-dependent absorptivity coefficient (also known as molar absorptivity), b is the cell-path length, and c is the analyte concentration.

$$A = \varepsilon bc \tag{1}$$

In terms of transmittance (T), which is defined as $T = I / Io$, where I is the light intensity after it passes through the sample, and Io is the initial light intensity. The relation between A and T is:

$$A = -\log T = -\log(I/Io) \tag{2}$$

Linear attenuation coefficient $\mu = \sigma C$ usually expressed in units of cm^{-1} and it is a function of wavelength.

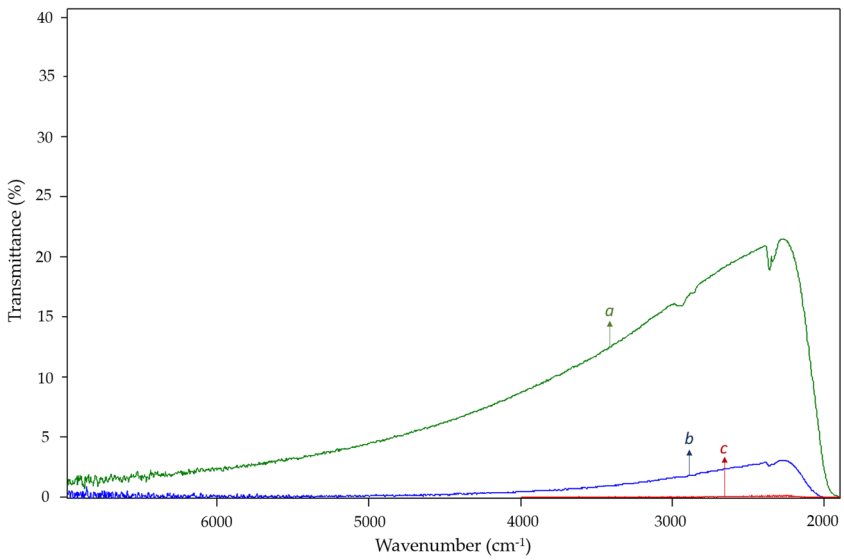

Fig. 4 Comparison of FTIR results of Y/La2010 sample for different thickness: a—green, 0.3 mm; b—blue, ~0.8 mm; c—red, ~2.6 mm

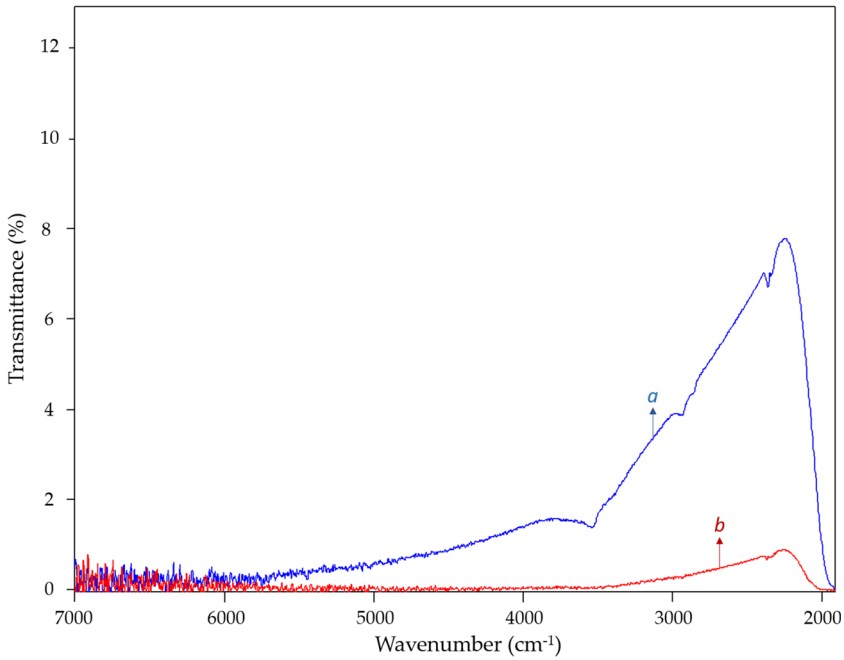

Fig. 5 Comparison of FTIR results of Dy/La2010 sample for different thickness: a—blue, ~ 0.3 mm; b—red, ~ 0.8 mm

$$I = I_0 e^{-\mu m} \tag{3}$$

where m is the path length of the sample. As the definition of law, the intensity of light decreases exponentially with depth in the material. According to the results shown in Table 3, transmission through the samples increased by reduction of sample thickness which is consistent with Beer-Lambert Law.

The FTIR graphs of the Y/La2010 and Dy/La2010 samples were shown in Figs. 4 and 5, respectively. An additional absorption peak in the Dy^{3+} doped sample (Dy/La2010) was determined at 3540 cm^{-1} which belongs to the electron transmission of $6H_{15/2} \rightarrow 6H_{11/2}$ [23]. Due to this reason, this absorption peak was not observed FTIR graph of Y/La2010 sample. It is notable that at every sample thickness IR transmission of Y/La2010 was performed better than Dy/La2010. Furthermore, the infrared transmission percent of the YLa2010 sample was found as three times higher than that of Dy/La2010 (for 0.3-mm sample thickness). In our previous works, we reported that the primary parameters that determined the optical properties of α-SiAlON ceramics are density, microstructural homogeneity, phase variety, and grain size/shape [17, 30]. Additive cations have a strong influence on these properties of SiAlON ceramics and therefore indirectly affect the transmission performance at IR and visible wavelength. In addition, since the additive cations can enter the α-SiAlON crystal structure, they change the electronic and optical gap. So, the choice of dopants plays a decisive role in α-SiAlON ceramics transmission. The variation of the refractive index of AlN-polytype, α-SiAlON, and glassy phase in the multi-component SiAlON structure cause reduction in transmission. According to the SEM micrographs, the amount of glassy phase and its distribution in the Y/La2010 sample is relatively lower and homogeneous than that of Dy/La2010. This observation indicates that for co-doped α-SiAlON ceramics, which is La^{3+}-Y^{3+} cation system promotes incorporation higher amount of additive cations into the α-SiAlON structure. This behavior results in the reduction of the glassy phase and provides microstructural homogeneity, so it improves the infrared transmission of α-SiAlON. Dy/La2010 also includes more amount of elongated and coarser α-SiAlON grains (Fig. 2(a), point 2) than Y/La2010; this formation might be another reason of relatively lower transmission value of Dy/La2010 than Y/La2010.

Few studies in the literature reported the optical properties of co-doped α-SiAlON ceramics. It has been published that Dy/Y-α-SiAlON ceramics could reach 50–65% IR transmission by optimization of sintering parameters or applying heat treatment after the sintering stage to tailor microstructure [31, 32]. Joshi et al. fabricated 100-μm-thick Mg/Eu-α/β-SiAlON ceramics with more than 60% transmission in the range between 200 and 1000 nm [33]. In this study, co-dopped α-SiAlON ceramics with Dy/La and Y/La could not reach the same amount of IR transmission due to the microstructural inhomogeneity, phase variety, and elongated grain morphology. However, the existence of elongated grains and AlN-polytypes might be useful for some applications which require improved mechanical properties besides IR transmission. Co-doping α-SiAlON ceramics with Dy/La and Y/La cation systems may not give the best IR transmission performance but have a potential for further studies to obtain IR-translucent α-SiAlON ceramics with relatively high fracture strength and toughness.

Conclusions

In this study, translucent co-dopped Dy/La-SiAlON and Y/La-SiAlON ceramics successfully fabricated by using spark plasma sintering technique. Both of the samples contain mainly α-SiAlON phase with a little amount of AlN-polytype. Although a cation with a large ionic radius such as lanthanum was used, no phase transformation from α-SiAlON to β-SiAlON occurred. When compared with Dy^{3+}/La^{3+} system, coupling La^{3+} with Y^{3+} were provide better support for the incorporation of cations into the structure and, so the reduction of the glassy phase. Due to the existence of the lower amount of glassy phase and, elongated α-SiAlON grains in Y/La-α-SiAlON sample, this sample was showed three times higher infrared transmission than that of Dy/La-α-SiAlON. The results showed that the presence of secondary phases such as AlN-polytype and glassy phase affects the optical properties of α-SiAlON ceramics negatively. Therefore, it is showed that by selecting the correct additive cation combination, it is possible to produce α-SiAlON ceramics with high optical and infrared transmittance.

Funding information This study received financial support from The Scientific & Technological Research Council of Turkey (Project: 111M427).

References

1. He, W., Liu, Q., Zhong, H.: Composition controlled microstructure and mechanical properties of Yb/Lu co-doped SiAlON. Mater. Sci. and Eng A. **528**, 8359–8364 (2011)
2. Chen, W., Shuba, R.A., Zenotchkine, M.Y.: Development of tough alpha-SiAlON. Key Eng. Mater. **237**, 65–78 (2003)
3. Huang, Z.K., Rosenflanz, A., Chen, I.W.: Pressureless sintering of Si_3N_4 ceramic using AlN and rare-earth oxides. J. Am. Ceram. Soc. **80**(5), 1256–1262 (1997)
4. Mandal, H., Hoffmann, M.J.: Preparation of multiple-cation α-SiAlON ceramics containing lanthanum. J. Am. Ceram. Soc. **82**(1), 229–232 (1999)
5. Shen, Z. J., Nordberg, L. O., Nygren, M., Ekstrom, T.: α-SiALON grains with high aspect ratio-utopia or reality. Engineering Ceramics'96: Higher Reliability Through Processing. **25**, 169–178 (1997)
6. Huang, Z.K., Jiang, Y.Z., Tien, T.Y.: Formation of α-SiAlON with dual modifying cations (Li+Y and Ca+Y). J. Mater. Sci. Lett. **16**, 747–751 (1997)
7. Nordberg, L.O., Shen, Z., Nygren, M., Ekstrom, T.: On the extension of the α-SiAlON solid solution range and anisotropic grain growth in Sm-doped α-SiAlON ceramics. J. Eur. Ceram. Soc. **17**, 575–580 (1997)
8. Krell, A., Klimke, J., Hutzler, T.: Advanced spinel and sub-m Al_2O_3 for transparent armour applications. J. Eur. Ceram. Soc. **29**, 275–281 (2009)
9. Krell, A., Hutzler, T., Klimke, J.: Transmission physics and consequences for materials selection, manufacturing, and applications. J. Eur. Ceram. Soc. **29**, 207–221 (2009)
10. Karunatne, B.S.B., Lumby, R.J., Lewis, M.H.: Rare-earth-doped α-SiAlON ceramics with novel optical properties. J. Mater. Res. **11**(11), 2790–2794 (1996)
11. Jones, M.I., Hyuga, H., Hirao, K.: Optical and mechanical properties of α/β-SiAlON composites. J. Am. Ceram. Soc. **86**(3), 520–522 (2003)
12. Jones, M.I., Hyuga, H., Hirao, K., Yamauchi, Y.: Highly transparent Lu-α-SiAlON. J. Am. Ceram. Soc. **87**(4), 714–716 (2004)
13. Yingchun, S., Jiujun, X., Chunlong, G., Jiangtao, L.: Preparation and properties of translucent Y-α-Sialon ceramics by two-steps hot pressing. Key Eng. Mater. **434-435**, 661–663 (2010)
14. Su, X.L., Wang, P.L., Chen, W., Zhu, B., Cheng, Y., Yan, D.: Translucent α-SiAlON ceramics by hot pressing. J. Am. Ceram. Soc. **87**, 730–732 (2004)
15. Xiong, Y., Fu, Z., Wang, Y.H., Wang, Y.C., Zhang, J.Y., Zhang, Q.J.: Translucent Mg-α-SiAlON ceramics prepared by spark plasma sintering. J. Am. Ceram. Soc. **90**, 1647–1649 (2007)
16. Qian, L., Wei, H., Hongmei, Z., Kun, Z., Linhua, G.: Transmittance improvement of Dy-α-SiAlON in infrared range by post hot-isostatic-pressing. J. Eur. Ceram. Soc. **32**, 1377–1381 (2012)
17. Avcioglu, S., Kurama, S.: Investigation of the influence of initial powder size on the optical properties of Dy-α-SiAlON ceramics fabricated by gas pressure sintering. Ceram. Int. **43**, S449–S454 (2017)
18. Xiong, Y., Fu, Z.Y., Wang, H., Wang, Y.C., Zhang, J.Y., Zhang, Q.J.: Microstructure and properties of translucent Mg–sialon ceramics prepared by spark plasma sintering. Mater. Sci. Eng. A. **488**, 475–481 (2008)
19. Feng, Y., Limeng, L., Chunfeng, L., Haijiao, Z., Yu, Z., Jie, Y.: High infrared transmission of Y^{3+}–Yb^{3+} doped α-SiAlON. Mater. Lett. **62**, 4535–4538 (2008)
20. Mandal, H.: New developments in α-SiAlON ceramics. J. Eur. Ceram. Soc. **19**, 2349–2357 (1999)
21. Shen, Z.J., Nygren, M., Hslenius, U.: Absorption spectra of rare-earth-doped α-SiAlON ceramics. J. Mater. Sci. Lett. **16**, 263–266 (1997)
22. Liu, L., Ye, F., Zheng, S., Peng, B.L.W., Zhang, Z., Zhou, Y.: Light transmittance in α-SiAlON ceramics: effect of composition, microstructure, and refractive index anisotropy. J. Eur. Ceram. Soc. **32**, 2487–2494 (2012)
23. Zhong, H.M., Liu, Q., Jiang, J., Sun, G.Y., Luo, Y.: A first principles study on optical transparency mechanism in Dy doped α-SiAlON ceramics. J. Appl. Physiol. **106**(9), 093514 (2009)
24. Hewett, C.L., Cheng, Y.B., Muddle, B.C.: Phase relationships and related microstructural observations in the Ca-Si-Al-O-N system. J. Am. Ceram. Soc. **81**(7), 1781–1788 (1998)
25. Zhao, R., Swenser, S.P., Cheng, Y.B.: Formation of AlN-polytypoid phases during α-SiAlON decomposition. J. Am. Ceram. Soc. **80**(9), 2459–2463 (1997)
26. Chen, W., Sun, W., Li, Y., Yan, D.: Approach for improving homogeneity of Ln-α-sialon–AlN-polytypoid composite ceramics. Mater. Lett. **44**, 181–185 (2000)
27. Menon, M., Chen, I.-W.: Reaction densification of α′-SiAlON: 1 wetting behavior and acid-base reactions. J. Am. Ceram. Soc. **78**(3), 545–552 (1995)
28. Menon, M., Chen, I.-W.: Reaction densification of α′-SiAlON: II, densification behavior. J. Am. Ceram. Soc. **78**, 553–559 (1995)
29. Li, H.X., Sun, W.Y., Yan, D.S.: Fabrication and mechanical properties of α'-sialon-12H Multi Phase Ceramics Proc. 5th Inter. Symp. on Ceramic Materials and Components for Engines. World Scientific. 194–197 (1995)
30. Kurama, S., Avcioglu, S., Ayas, E.: Optimization of the optical properties of α-SiAlON through a decrease in starting powder size. J. Eur. Ceram. Soc. **35**, 3229–3235 (2015)
31. Avcioglu, S., Kurama, S.: Spark plasma sintering of translucent Dy–Y doped α-SiAlON: study of sintering parameters influence

on the optical properties by using Taguchi method. Acta Phys. Pol. A. **131**(1), 174–177 (2017)

32. Xinlu, S., Peiling, W., Weiwu, C., Zhijian, S., Nygren, M., Yibing, C., Dongsheng, Y.: Optical properties of SPS-ed Y- and (Dy,Y)-α-sialon ceramics. J. Mater. Sci. **39**, 6257–6262 (2004)
33. Bhupendra, J., Yuwaraj, K.K., Gobinda, G., Soo, W.L.: Transparent Mg-α/β-Sialon:Eu^{2+} ceramics as a yellow phosphor for pc-WLED. J. Alloys Compd. **631**, 38–45 (2015)